On the Enclathration of $NaB(OH)_4$ in the β-Cages of Sodalite: Crystallization Kinetics and Crystal Structure

J.-Ch. Buhl, C. Mundus*, J. Löns, and W. Hoffmann

Institute of Mineralogy, University of Münster, Corrensstr. 24, D-48149 Münster
(Federal Republic of Germany)
* Institute of Physical Chemistry, University of Münster, Schloßplatz 4, D-48149 Münster
(Federal Republic of Germany)

Z. Naturforsch. **49a**, 1171–1178 (1994); received September 26, 1994

Dedicated to Professor Werner Müller-Warmuth on the occasion of his 65th birthday

The hydrothermal formation of sodium hydroxyborate enclathrated sodalite synthesized from an initial ternary mixture of mullite, cristobalite and corundum has been investigated. Depending on temperature and pressure the compound $Na_{7.5}[AlSiO_4]_6[B(OH)_4]_{1.5} \cdot 2\,H_2O$ could be synthesized in form of polycrystalline powder as well as in form of single crystals. The kinetics of the sodalite growth could be determined at 423 K and 473 K. ^{29}Si- and ^{27}Al MAS NMR was shown to be the preferred method to describe the conversion into sodalite quantitatively. Evidence for the first formation of polycrystalline sodalite has been found after the total dissolution of mullite and cristobalite.

Single crystal X-ray diffraction data were used for the structure determination and refinement. The position and orientation of the hydroxyborate anions within the sodalite's β-cages could only be found in the course of a "rigid body" refinement with constraints for the $B(OH)_4$ tetrahedron. The boron atoms are located in an off-centre position within the sodalite cages. One out of the four oxygen atoms of the hydroxyborate group is positioned near the centre of a face of the sodium tetrahedron, whereas the three remaining oxygen atoms are near to the middle of its edges.

Key words: Sodalite solid solution, Crystallization kinetics, IR-spectroscopy, MAS NMR, Structure refinement.

Introduction

The aluminosilicate framework of the sodalite structure formed by the space-filling array of $[4^6 6^8]$ polyhedral cages, the so-called β-cages, can be regarded as a nanoporous matrix with well defined openings for the enclathration of guest molecules. New promising applications of sodalites have recently been proposed on this basis. Their use as nanocomposites in nonlinear optics or for host matrices of semiconductor quantum superlattices (Stein et al. [1, 2]) as well as for waste gas immobilisation (Buhl [3]) should be mentioned here. Such utilizations require crystalline material of very high quality. The synthesis should lead to a product of a narrow crystal size distribution, to a framework topology of the crystals without stacking faults, and to a homogeneous distribution of the guest molecules within the crystals. The quality of crystals in this sense already depends on the crystallization process in its very early stage. Buth with regards to this initial period of phase formation many open questions exist, especially for the hydrothermal method of crystallization, which is the only suitable way to grow sodalites with temperature-sensitive templates.

To extend the knowledge on the formation of salt enclathrated sodalites we report here the results of large-scale investigations on the crystallization kinetics and structure determination of sodium hydroxyborate containing sodalite, a borate filled compound with interesting properties (Barrer and Freund [4], Buhl et al. [5]). Earlier investigations have already shown that the nucleation process of sodalite is highly influenced by the nature of the starting materials (Denk and Menzel [6], Hayashi et al. [7], Subotic et al. [8, 9], Buhl et al. [10]). For our experiments a mixture of three oxides, obtained by sintering from p.a. chemicals, has been used as an educt. It should be mentioned that instead of the most common educt kaolinite very pure chemicals must be used to improve the crystal quality.

The investigations on the crystallization kinetics as well as on the crystal structure of the hydroxyborate sodalite have been carried out by X-ray powder dif-

---

Reprint requests to Dr. J.-Ch. Buhl.

0932-0784 / 94 / 1200-1171 $ 06.00 © – Verlag der Zeitschrift für Naturforschung, D-72027 Tübingen

Table 1. The results of the hydrothermal syntheses according to X-ray powder diffraction.

No.	Temperature (K)	Time (h)	Products**
1	423	t_0*	M+Cr+Co
2	423	t_0+1	M+Cr+Co
3	423	t_0+24	Hbs+Co+(M)+(Cr)
4	423	t_0+48	Hbs+Co+(M)+(Cr)
5	423	t_0+72	Hbs+Co
6	423	t_0+96	Hbs+Co
7	473	t_0*	M+Cr+Co
8	473	t_0+1	Hbs+Co+(M)+(Cr)
9	473	t_0+24	Hbs
10	473	t_0+48	Hbs
11	473	t_0+72	Hbs
12	473	t_0+96	Hbs

* t_0: time until the autoclaves reached the reaction temperature.
** M: mullite, Cr: cristobalite, Co: corundum, Hbs: hydroxyborate sodalite, ( ): small amounts.

Table 2. The time-dependend conversion of the educts to hydroxyborate sodalite at 423 K and 473 K according to ^{27}Al MAS NMR spectra integration.

t (h)	Hydroxyborate sodalite in percent	
	Reaction at 423 K	Reaction at 473 K
t_0	0	0
t_0+1	0	30
t_0+24	18	91
t_0+48	26	93
t_0+72	39	92
t_0+96	49	100.0

fraction, simultaneous thermal analysis, IR-spectroscopy, ^{29}Si- and ^{27}Al-MAS NMR and single crystal X-ray diffraction.

Experimental

The hydrothermal syntheses of hydroxyborate sodalite were performed in 50 ml teflon coated steel autoclaves, filled with 2 g of a homogeneous mixture of 21 wt% mullite ($Al_6Si_2O_{13}$), 48 wt% cristobalite (SiO_2) and 31 wt% corundum (Al_2O_3). This starting material could be obtained from γ-Al_2O_3 (Merck 1095) and SiO_2 (Merck 657) mixed in a 1:1 molar ratio and heated for two hours at 1673 K. Together with 45 ml of an 8-molar NaOH solution (Merck 6495) an additional amount of 5.6 g of boric acid (Merck 765) has been added. The $B(OH)_4^-$ anions were always obtained from $B(OH)_3$ under the highly alkaline conditions used in the experiments (Ingri [11]). Two reaction temperatures (423 K and 473 K) were selected to study the crystallization kinetics of hydroxyborate sodalite up to a reaction time of 96 h. All products were washed with 150 ml of distilled water and dried for 24 h at 353 K. Subsequently the obtained products were characterised by X-ray powder diffraction (Guinier-Jagodzinski camera, Cu-Kα radiation, internal Si-standard), by simultaneous thermal analysis (Mettler Thermoanalyzer TA 146) and by IR-spectroscopy (Perkin Elmer Spectrometer 683, using KBr-pellets).

The crystal phases formed during syntheses were determined by X-ray powder diffraction. The filling of the sodalite cages with the guest species was checked by thermogravimetry in connection with IR-spectroscopy. The borate content of selected samples was analysed spectralphotometrically using the micromethod described by Gupta and Boltz [12].

A Bruker CXP-300 FT NMR spectrometer with a MAS-probehead has been used to obtain the ^{29}Si- and ^{27}Al MAS NMR spectra of the reaction products. The ^{29}Si MAS NMR spectra were recorded at 59.5 MHz using a single pulse sequence with 2–3 μs pulse duration and 3–7 s pulse delay and a spinning rate of 4 kHz. Chemical shifts were related to the tetramethylsilane standard. ^{27}Al MAS NMR spectra were obtained at a resonance frequency of 78.2 MHz, with 3.7–5 μs pulse duration and 5–10 s pulse delay and with 4.5–6 kHz spinning rate. A 1-molar solution of $AlCl_3$ has been taken as internal standard for chemical shifts.

Single crystal syntheses were carried out under temperature and pressure conditions of 573 K and 0.1 GPa for 120 h in Bridgman steel autoclaves of 18 ml volume as described by Buhl et al. [5]. Silver liners 80 mm in length and 8 mm in diameter were filled with 50 mg of the sintered educt together with 280 mg of boric acid and 1 ml of an 8-molar NaOH solution. The autoclaves were heated in a vertical cylindrical furnace with 573 K at the bottom of the autoclave under a temperature gradient of 2 K/cm. The pressure of 0.1 GPa, estimated from the Kennedy diagram [13], was controlled by the degree of the autoclave's filling.

A dodecahedral shaped crystal of 0.45 mm in diameter was selected for the single crystal diffraction measurements with an ENRAF-NONIUS four circle diffractometer CAD 4. Precession photographs show reflections consistent with the space group symmetry

Table 3. Crystallographic data and experimental conditions for structure refinement of hydroxyborate sodalite.

Crystal size and shape	0.45 mm, dodechedral
Data collection:	
Mo Kα radiation (graphite monochromator)	
Temperature	295 K
Cell parameter calculated from 25 reflections in the 2θ-range of 4°–60°	$a_0 = 9.024\ (1)$ Å
Space group	$P\bar{4}3n$
Number of reflections	16511
8525 reflections in the 2θ-range and range of reciprocal space	$4° \leq 2\theta \leq 60°$: $-17 \leq h \leq 17$ $-17 \leq k \leq 17$ $-7 \leq l \leq 7$
7986 reflections in the 2θ-range and range of reciprocal space	$60° \leq 2\theta \leq 120°$ $0 \leq h \leq 25$ $0 \leq k \leq 25$ $-10 \leq l \leq 10$
Number of reflections after Data reduction	1414 [$I > 3$ sigma(I)]
Internal R-value:	2.1%
R-value (unweighted):	2.4%
R-value (weighted):	2.1%
Number of refined parameters	63

$P\bar{4}3n$. The experimental details are summarized in Table 3.

For all structural refinement calculations the program SHELX [14] has been used. The atomic scattering factors for neutral atoms were taken from the International Tables [15], whereas the initial positional parameters were chosen from the single crystal refinement of NaCl sodalite [16].

Results

The products of synthesis, removed from the autoclaves after different length of time up to 96 hours $+ t_0$ (t_0: time needed for heating up the autoclave to the reaction temperature) were obtained as white polycrystalline powders. The compositions as they were found by the analysis did not differ significantly from $Na_{7.5}[AlSiO_4]_6[B(OH)_4]_{1.5} \cdot 2\,H_2O$. The results of the phase analyses by X-ray powder diffraction are summarized in Table 1; all the X-ray powder diagrams are well known from the literature (Buhl et al. [5]; JCPDS [17]). Besides remaining amounts of the initial substances, which decrease with increasing reaction time, sodalite is the one and only compound formed in the hydroxyborate system. Such a direct formation of sodalites from the educts is also observed for the sodalite synthesis from Zeolite A (Subotic et al. [8, 9]) as well as from kaolinite (Buhl et al. [10]); only in case of the synthesis of basic sodalite from gels (Hayashi et al. [7]). The crystallization of an intermediate phases has become known.

From the results of the X-ray powder diffraction experiments in Table 1 the progress of the reactions can be estimated qualitatively. But it is not simply possible to receive the quantitative amounts of sodalite and the three initial compounds without very much effort to obtain accurate results.

Other attempts were made to use simultaneous thermal analysis for the qualitative and quantitative description of the crystallization process. Figure 1 shows the results of differential thermogravimetry (DTG) and differential thermoanalysis (DTA) for two selected products out of the series of experiments at 473 K. Only for reactions longer than 72 hours the behaviour during thermoanalysis corresponds with that of hydroxyborate sodalites as a single phase (Buhl and Luger [18]). After shorter times as well as at lower temperatures thermal analysis cannot be used for getting proper informations on the progress of the reaction due to high amounts of water released from amorphous material as it is already known from the investigation of sodalite formation using kaolinite as starting material (Buhl et al. [10]).

Besides X-ray powder diffraction, IR spectroscopy can also be used for the qualitative identification of the synthesized phases according to their characteristic absorption bands. But the results from the IR measurements clearly show that such a qualitative phase analysis is only possible for the nearly pure products obtained after the long time hydrothermal runs at 473 K. Because of various overlappings of characteristic absorption bands of mullite, cristobalite, corundum and sodalite mainly in the 1200 cm^{-1}–600 cm^{-1} range (Moenke [19]) it is impossible to distinguish between these phases during stages of incomplete reaction as shown in Figure 2a. In contrast Fig. 2b shows clearly resolved T-O-T vibration bands of sodalite (Henderson and Taylor [20]) prepared as a single phase at the elevated temperature. The enclathrated $B(OH)_4$ anion can only be detected by its strong OH^- vibration band at 3640 cm^{-1}.

MAS NMR of the ^{29}Si and ^{27}Al nucleus has been proved to be a much better tool for phase analysis as well as for the quantitative determination of the reaction progress (Buhl et al. [10]). The ^{29}Si and ^{27}Al MAS NMR spectra obtained from the products of syntheses at 423 K and 473 K are shown in Figs. 3a and 3b. The initially inserted substances and sodalite as the reaction product can be clearly distinguished according to

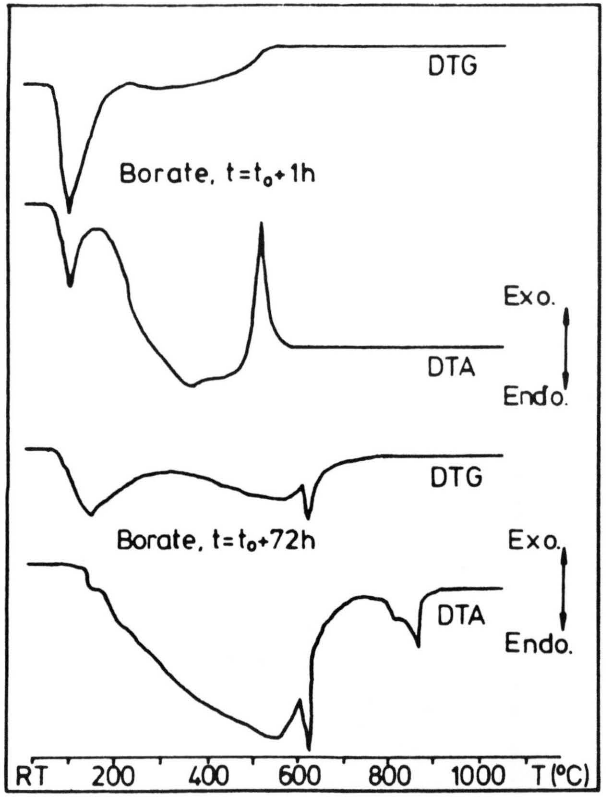

Fig. 1. The results of differential thermogravimetry (DTG) and differential thermoanalysis (DTA) for two selected products from syntheses at 473 K.

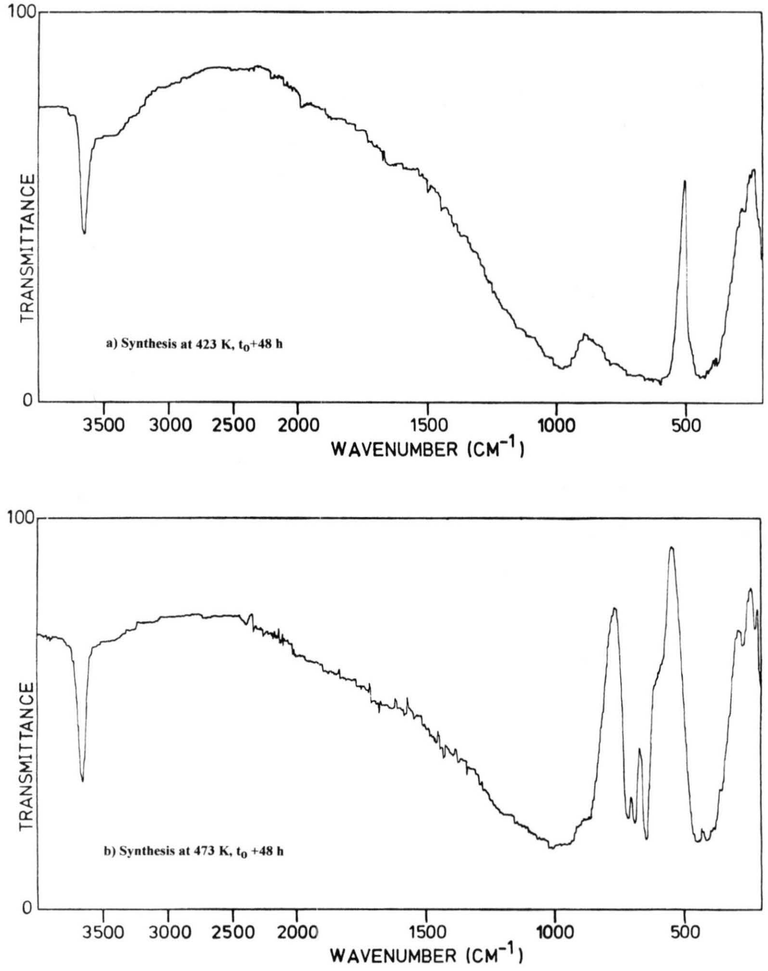

Fig. 2. IR-spectra of two selected products: a) Synthesis at 423 K for 48 h; b) Synthesis at 473 K for 48 h.

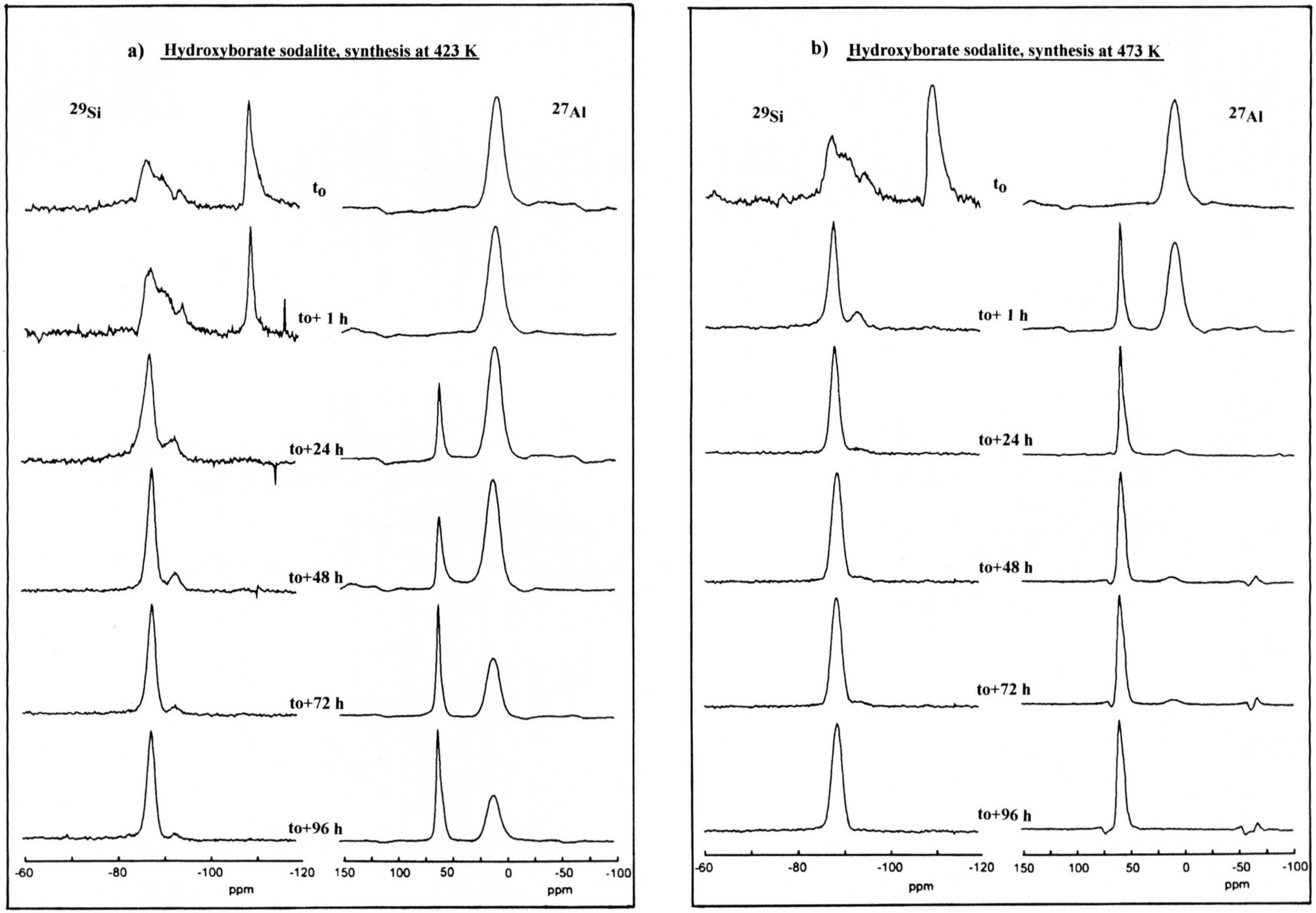

Fig. 3. The ^{29}Si- and ^{27}Al MAS NMR spectra of the reaction products: a) Syntheses at 423 K; b) Syntheses at 473 K.

their different chemical shifts: cristobalite at $\delta_{iso}{}^{29}Si = -109$ ppm (Mägi et al. [21]; Smith et al. [22]), mullite at $\delta_{iso}{}^{29}Si = -80$ ppm and -95 ppm and hydroxyborate sodalite at $\delta_{iso}{}^{29}Si = -88.5$ ppm (Buhl et al. [10]) and $\delta_{iso}{}^{27}Al = 63.4$ ppm, corundum and mullite at $\delta_{iso}{}^{27}Al = 10.1$ ppm (Jacobson et al. [23]). Taking into account the qualitative results of the X-ay phase analysis the sodalite formation from the mixed oxides can be easily obtained quantitatively by peak integration from the ^{27}Al MAS NMR signals. The results are summarized in Table 2. The conversion of phases obtained for the synthesis at 423 K show a remarkable low reaction rate as compared with the sodalite crystallization from other initial compounds like zeolite A (Subotic et al. [8, 9]) or kaolinite (Buhl et al. [10]). Whereas 100% conversion to sodalite could already be obtained after 24 h using the single phase educts zeolite A and kaolinite even at 353 K, $96\,h + t_0$ at 423 K gave only 49% of sodalite from the ternary mixture of oxides; 100% conversion could only be obtained after $96\,h + t_0$ at the higher temperature of 473 K. It can be seen from both the ^{29}Si and ^{27}Al NMR spectra that there are suspicious differences in the hydrothermal solubility of slightly soluble corundum on the one hand and easily but likely soluble cristobalite and mullite on the other hand. The first formation of polycrystalline sodalite becomes obvious after the total dissolution of mullite and cristobalite.

The strong peak of the ^{29}Si NMR spectra of all synthesized sodalites clearly indicates the alternating ordering of Si and Al atoms in the overwhelming part of the sodalite framework (Si[4Al] units) and a Si/Al ratio close to one. There is, however, another very weak peak at -93.5 ppm in the spectra, which has to be assigned to Si(3Al) units indicating the replacement of a very small amount of Al atoms by Si atoms. In this respect ^{29}Si MAS NMR spectroscopy is a much more sensitive method than the above mentioned chemical analysis.

The single crystals of hydroxyborate sodalite grown at higher temperature and pressure have the same chemical composition $Na_{7.5}[AlSiO_4]_6[B(OH)_4]_{1.5} \cdot 2\,H_2O$, the same lattice constant ($a_0 = 9.024(1)$ Å) and the same strong Si, Al-order as the material synthesized in the form of powders. Structure determination and refinement with these single crystals therefore can answer the open question, how the $B(OH)_4^-$-tetrahedra are arranged inside the sodalite's β-cages. As already mentioned above, structural refinement in the space group $P\bar{4}3n$ started with the atomic coordinates of NaCl-sodalite but replacing the Cl^- in the centre of the β-cages by boron. The boron is surrounded by the four oxygen atoms of the OH^--groups distributed on the 24-fold general position (24i) in the sense of positional disorder. In addition, four nearly independent positions for the sodium cations were found on the diagonals of the cubic cell (each on 8e in $P\bar{4}3n$) close to the six-membered rings of the β-cages. These split positions of different occupancy as well as the deficiency of sodium ions (7.5 Na^+ per unit cell) can be explained as a result of $[Na_4 \cdot B(OH)_4]^{3+}$ and $[Na_3 \cdot (H_2O)_4]^{3+}$ cage fillings randomly distributed in the crystals and a deviation of the tetrahedral hydroxyborate groups from cubic orientation, breaking the point symmetry 23 in the centre of the cages. Orientational disorder of these anionic groups, tantamount to the positional disorder of the appropriate oxygen atoms, lead to the high symmetry $P\bar{4}3n$ of the average structure.

The refinement converged at $R_W = 0.026$, but despite the goodnes of fit between the calculated and the observed structure factors the interatomic distances and angles of the imbibed guest anions showed major deviations from the geometry of this group in solid $NaB(OH)_4$ (B–O-distance: 1.472 Å, Ketterer [24]). Because of these deviations the single tetrahedral hydroxyborate group and its orientation could not be recognized. Thus, for a better determination of the guest anions within the sodalite cages an extended refinement using constraints for the bond distances and angles of the hydroxyborate group was carried out. Considering $B(OH)_4^-$ as a "rigid body" with regular geometry as found in solid $NaB(OH)_4$, the correct position of this group inside the sodalite cages could be discovered.

The final atomic parameters including positions, site occupancies and isotropic temperature coefficients of this "rigid-body" refinement are given in Table 4. It turns out that the boron atom is shifted significantly from the centre of the β-cage. The refined site occupancies give a chemical composition of the crystal $Na_{7.6}[AlSiO_4]_6[B(OH)_4]_{1.6} \cdot 1.9\,H_2O$ in very good agreement with chemical analysis.

Selected interatomic distances and bond angles are summarized in Table 5. The framework of hydroxyborate sodalite consists of completely ordered AlO_4 and SiO_4 tetrahedra with a Si–O–Al angle of 144.1(1)° and a Si/Al ratio of 1.0. This angle as well as the lattice constant is in good agreement with corresponding values obtained from the correlation function with the

Table 4. Fractional atomic coordinates, site occupancies and equivalent displacement parameters of hydroxyborate sodalite (e.s.d.'s are given in parentheses).

Atom	Site	Occupancy	x	y	z	U_{eq}*
Aluminosilicate framework						
Si	6d	1.0	0.250	0.000	0.500	0.0070 (1)
Al	6c	1.0	0.250	0.500	0.000	0.0070 (1)
O1	24 i	1.0	0.1422 (1)	0.4523 (1)	0.1522 (1)	0.0158 (1)
Na1	8 e	0.499	0.1827 (2)	0.1827 (2)	0.1827 (2)	0.0270 (4)
Na2	8 e	0.152	0.2038 (5)	0.2038 (5)	0.2038 (5)	0.0204 (6)
Na3	8 e	0.180	0.2274 (6)	0.2274 (6)	0.2274 (6)	0.0343 (7)
Na4	8 e	0.113	0.1963 (11)	0.1963 (11)	0.1963 (11)	0.0174 (8)
$B(OH)_4^-$-anion**						
B	24 i	0.0702 (6)	−0.0755 (5)	0.0028 (6)	−0.0256 (5)	0.021 (1)
O21	24 i	0.0702 (6)	0.0363 (8)	0.1592 (7)	−0.0462 (9)	0.024 (1)
O22	24 i	0.0702 (6)	0.0503 (9)	−0.0868 (9)	−0.1497 (8)	0.112 (1)
O23	24 i	0.0702 (6)	−0.1708 (5)	0.0080 (9)	−0.0219 (7)	0.018 (1)
O24	24 i	0.0702 (6)	0.0541 (9)	−0.0530 (10)	0.1154 (7)	0.043 (2)
Water molecules						
O3	24 i	0.0821 (2)	0.431 (1)	0.423 (2)	0.395 (2)	0.256 (1)

* ($U_{eq} = (1/24\pi^2) \sum_i \sum_j B_{ij} a_i^* a_j^* a_i a_j$. ** Isotropic refinement.

Table 5. Selected interatomic distances (Å) and angles (°) of hydroxyborate sodalite.

Framework			
Si–O1	1.616 (1)	Al–O1	1.738 (1)
O1–Si–O1 (2×)	113.8 (0)	O1–Al–O1 (2×)	111.9 (0)
O1–Si–O1 (4×)	107.4 (0)	O1–Al–O1 (4×)	108.3 (0)
Si–O1–Al	144.1 (0)		
Na coordination			
Na1–O1	2.475 (2)	Na2–O1	2.394 (6)
Na3–O1	2.368 (3)	Na4–O1	2.274 (2)
Na1–O21	2.461 (9)	Na1–O24	2.498 (9)
Na2–O23	2.435 (17)	Na3–O23	2.430 (11)
Na4–O23	2.435 (17)		
$B(OH)_4^-$-anion			
B–O21	1.477 (8)		
B–O22	1.477 (9)	O21–B–O22	109.5 (5)
B–O23	1.477 (7)	O21–B–O23	109.5 (5)
B–O23	1.477 (8)	O22–B–O23	109.5 (5)
		O24–B–O21	109.5 (5)
		O24–B–O22	109.5 (5)
		O24–B–O23	109.5 (5)

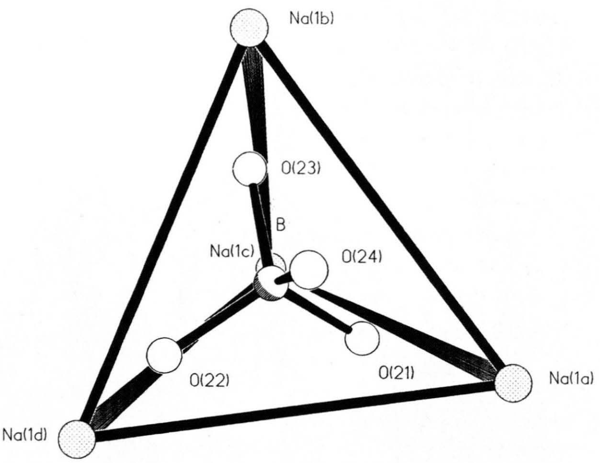

Fig. 4. The position of the $B(OH)_4^-$ group within the tetrahedral arrangement of the sodium cations (the split positions of the Na-cations are not drawn).

^{29}Si MAS NMR chemical shift (Engelhardt et al. [25]).

The position of the hydroxyborate anion within the tetrahedral arrangement of the sodium cations in each sodalite cage is shown in Fig. 4 (the non-equivalent split positions of the sodium cations are neglected in this figure). One out of the four oxygen atoms of the hydroxyborate group is positioned near the centre of a face of the sodium tetrahedron, whereas the three remaining oxygen atoms are near to the middle of its edges. Further experiments like neutron diffraction and scattering are necessary to find the hydrogen positions and to clarify the transition from static to dynamic orientation of the $B(OH)_4$-tetrahedron.

For the imbibed water molecules only the average positions were found, which agree with the coordinates in pure hydrosodalite (Felsche et al. [26]).

Acknowledgements

We are greatfully indebted to Prof. Dr. J. Grobe for the permission to use the IR spectrometer in his laboratory and to Mrs. A. Breit for technical assistance.

[1] A. Stein, G. A. Ozin, and G. D. Stucky, J. Amer. Chem. Soc. **112,** 904 (1990).

[2] A. Stein, G. A. Ozin, and G. D. Stucky, J. Amer. Chem. Soc. **114,** 8119 (1992).

[3] J.-Chr. Buhl, J. Solid State Chem. **94,** 19 (1991).

[4] R. M. Barrer and E. F. Freund, J. Chem. Soc. Dalton **1974,** p. 1049.

[5] J.-Chr. Buhl, G. Engelhardt, and J. Felsche, Zeolites **9,** 40 (1989).

[6] G. Denk and W. Menzel, Z. anorg. allg. Chem. **382,** 209 (1971).

[7] S. Hayashi, K. Suzuki, S. Shin, K. Hayamizu, and O. Yamamoto, Chem. Phys. Let. **110,** 54 (1984).

[8] B. Subotic, D. Skrtic, J. Smit, and L. Sekovanic, J. Cryst. Growth **50,** 498 (1980).

[9] B. Subotic and L. Sekovanic, J. Cryst. Growth **75,** 561 (1986).

[10] J.-Chr. Buhl, W. Hoffmann, W. A. Buckermann, and W. Müller-Warmuth, Europ. J. Miner. submitted 1994.

[11] N. Ingri, Svensk. Kem. Tidskr. **75,** 199 (1963).

[12] H. K. Gupta and D. F. Boltz, Microchimica Acta 415 (1974).

[13] G. C. Kennedy and W. T. Holser, Geol. Soc. Amer. Memoir. 97 (1966).

[14] G. M. Sheldrick, SHELX 76, Programm for Crystal Structure Determination, Cambridge 1976.

[15] International Tables for X-Ray Crystallography, Vol. 4, Kynoch Press, Birmingham 1974.

[16] J. Löns and H. Schulz, Acta Cryst. **23,** 434 (1967).

[17] JCPDS – International Centre for Diffraction Data, Powder Diffraction File, Sets 1–43 (1993).

[18] J.-Chr. Buhl and S. Luger, Thermochim. Acta **168,** 253 (1990).

[19] H. Moenke, Mineralspektren, Akademie-Verlag, Berlin 1962.

[20] C. M. B. Henderson and D. Taylor, Spektrochim. Acta **33 A,** 283 (1976).

[21] M. Mägi, E. Lippmaa, A. Samoson, G. Engelhardt, and A. R. Grimmer, J. Phys. Chem. **88,** 1518 (1984).

[22] J. V. Smith, R. J. Kirckpatrick, E. Oldfield, and D. M. Henderson, Amer. Mineral. **68,** 1206 (1983).

[23] H. J. Jakobsen, J. Skibsted, H. Bildsoe, and N. C. Nielsen, J. Magn. Res. **85,** 173 (1989).

[24] B. Ketterer, Dissertation Thesis, University of Konstanz (1988).

[25] G. Engelhardt, S. Luger, J.-Chr. Buhl, and J. Felsche, Zeolites **9,** 182 (1989).

[26] J. Felsche, S. Luger, and Ch. Baerlocher, Zeolites **6,** 367 (1986).